



Title	Correlation of quantum efficiency and photoluminescence lifetime of ZnO tetrapods grown at different temperatures
Author(s)	Tam, MC; Ng, AMC; Djuriscic, AB; Wong, KS
Citation	Journal of Applied Physics, 2012, v. 112 n. 2, article no. 023515
Issued Date	2012
URL	http://hdl.handle.net/10722/161507
Rights	Journal of Applied Physics. Copyright © American Institute of Physics.

Correlation of quantum efficiency and photoluminescence lifetime of ZnO tetrapods grown at different temperatures

M. C. Tam,¹ A. M. C. Ng,² A. B. Djurišić,² and K. S. Wong^{1,a)}

¹*Department of Physics, The Hong Kong University of Science and Technology, Hong Kong*

²*Department of Physics, The University of Hong Kong, Pokfulam Road, Hong Kong*

(Received 15 November 2011; accepted 27 June 2012; published online 23 July 2012; publisher error corrected 23 August 2012)

Absolute external quantum efficiencies (η_s) and photoluminescence (PL) decay lifetimes of ZnO tetrapods grown at different temperatures were measured. All the tetrapods had an UV peak at about 390 nm and a very weak defect emission. Measurements showed that the tetrapods have η_s of 2%–4% at room temperature. The sample, grown at optimal temperature, exhibited the largest absolute η of 4.3% and longest PL decay lifetimes among all the samples. These results showed that precise control of growth temperature plays an important role in making high quality ZnO tetrapods. In time-resolved measurement, the PL decay time constant (τ) versus temperature is well fitted by the theoretical prediction $\tau = aT^3$. This increase in PL lifetime with increasing temperature shows that the excited state relaxation is dominated by radiative recombination. © 2012 American Institute of Physics. [<http://dx.doi.org/10.1063/1.4737785>]

I. INTRODUCTION

In recent years, there is a huge interest in the study of ZnO. Due to its large band gap (~ 3.37 eV at 300 K) and large exciton binding energy (~ 60 meV), ZnO is a very promising material for UV emitter.^{1,2} Depending on its nanostructure, ZnO luminescence properties can be very different. For spontaneous emission at room temperature, ZnO usually has its photoluminescence (PL) peak around 380–390 nm, while defect emission can vary in the range 400–700 nm and depends strongly on impurities and native defects. Compared to other nanostructures such as nanorods and nanoshells, tetrapods have superior optical properties due to their strong UV and weak defect emission.^{2,3} In our previous work,⁴ ZnO tetrapods were grown in a narrow substrate temperature range for time-resolved PL study. The obtained PL lifetime for the optimal growth temperature was an order of magnitude higher than the best results achieved in epilayers and single crystals, while shorter PL lifetime and stronger defect emission were observed for both lower and higher growth temperatures. The exceptionally long PL lifetime for ZnO tetrapods was later confirmed by other group.⁵

We attempt to obtain further evidence for the enhanced emission at the optimal growth temperature. There were only few works on the measurements of the absolute quantum efficiencies of various ZnO nanostructures using an integrating sphere, such as crystalline nanowires and ZnO powder in different particle sizes.^{6–8} The advantage of using integrating sphere is that it eliminates the spatial variation of radiation of the sample and allows obtaining its absolute quantum efficiency. In this paper, absolute external quantum efficiencies of ZnO tetrapods grown at different temperatures were measured using an integrating sphere. A time-resolved experiment with the use of a streak camera was also carried out to measure the decay lifetimes of the tetrapods. For comparison, we

have also measured the quantum efficiency and decay lifetime of a ZnO crystal. In particular, we are interested in the temperature dependence of PL of tetrapods to investigate the origin of excited state recombination mechanism.

II. EXPERIMENTAL DETAILS

A. Fabrication

There were reports of how annealing temperature in furnace and type of gas flowing through the fabrication tube strongly affected the UV and defect emission of various ZnO nanostructures,^{9,10} which indicated these are also crucial factors other than nanostructure to control ZnO photoluminescence. ZnO tetrapods were fabricated in a horizontal tube furnace with temperature gradient by evaporating zinc at 950 °C in the flow of humid argon gas (0.2 Lpm) in air (quartz tube of 2 cm diameter with one open end). The humid argon gas was obtained by bubbling the argon gas through water before it passed into the furnace. Details of the fabrication process could be found in Ref. 4. The substrate temperature has a dramatic influence on the optical properties of ZnO tetrapods. Tetrapods grown in a very narrow temperature band around 915–930 °C exhibited strong UV emission with negligible defect emission, while defect emission appeared at temperatures slightly below (910 °C) or slightly above (940 °C). After fabrication, tetrapod powders were collected from the quartz tube and are divided into 4 different temperature regions. Powders were pressed as 4 tetrapod tablets, namely Z1 (lowest), Z2 (lower), Z3 (optimal), and Z4 (higher). Tetrapod sample Z3 was grown at the optimal temperature of ~ 930 °C, Z4 was grown at slightly higher temperature of ~ 940 °C, samples Z1 and Z2 were grown at lower temperature, approximately 15–20 °C lower than the optimal growth temperature. The ZnO crystal is Zn surface terminated and purchased from Cermet with dimension of 5×5 mm² and 1 mm thick.

^{a)}Author to whom correspondence should be addressed. E-mail: phkswong@ust.hk.

B. Integrating sphere measurement

The absolute external quantum efficiency, η , is defined by the ratio of the number of photons emitted from the tetrapod sample to the number of photons absorbed from the excitation source. The tetrapod sample was placed inside the integrating sphere, where light emission was redistributed isotropically over an interior surface coated with a diffusely reflecting material. The absolute quantum efficiency was obtained by integrating the measured PL signal over wavelength. A 325 nm CW light from a He-Cd laser was introduced into the integrating sphere to optically pump the sample. The excitation power was about 0.45 mW. An optical fiber collected the light from the sphere, and directed it to an Ocean Optics spectrometer. The response of the fiber and spectrometer/detector system was normalized by a standard light source.

The PL quantum yields were determined according to the method described by de Mello.¹¹ A standard technique for measuring thin-film PL quantum efficiencies with the use of an integrating sphere includes 3 measurements. For the first measurement, the sphere is empty and laser light (L_a) alone is detected. For the second measurement, the sample is placed inside the sphere and the laser beam is directed on to the sphere wall without directly hitting the sample. The detected signal is composed of scattered laser light from the sphere wall (L_b) and PL emitted after the absorption of scattered laser light (P_b). In the third measurement, the laser beam is directed onto the sample. After the sample absorbs both direct incident light and scattered light, there is a detected signal of laser light (L_c) and emitted PL (P_c). We assume the fraction of scattered light absorbed by the sample absorbed is μ and the fraction of incident light absorbed by the sample is A . The PL absolute external quantum efficiency of the tetrapod sample is

$$\eta = \frac{P_c - P_b(1 - A)}{L_a A} = \frac{P_c \cdot L_b - P_b \cdot L_c}{L_a(L_b - L_c)}. \quad (1)$$

The detailed derivation of this equation can be obtained in Ref. 11.

C. Time-resolved measurement

We also investigated the exciton lifetime and its correlation to the quantum efficiency in various samples using time-resolved PL measurements. For time-resolved measurement, a 76 MHz femtosecond Ti:sapphire oscillator was used as the excitation source and a streak camera coupled to a spectrometer was used as the detector. A pulse-picker was used to reduce the repetition rate of the laser to 4 MHz in order to measure accurately the long lived component of the ZnO PL lifetime. We carried out the room temperature measurement first for samples Z1-Z4 and ZnO crystal. The second harmonic of the Ti:sapphire oscillator was tuned to 355 nm in order to excite tetrapod samples which have UV emission peak around 390 nm. The excitation power was about 4 μ W. Temperature affects the quantum efficiency as well as the recombination rate. The temperature dependent time-resolved measurement was also carried out for Z3 and ZnO crystal. Each sample was cooled down to about 7 K and PL measurement was carried out with rising temperature until it reached 300 K.

III. RESULTS AND DISCUSSION

The time-integrated spectra of detected laser signals L_a , L_b , L_c , and PL signals P_b and P_c of Z3 are shown in Figure 1. The tetrapod powder tablets are not smooth but with slightly rough surface. PL intensity varies when the pumping laser hit on a different region on the tablet. Therefore, we measured the emitted PL (P_c) of 5 different regions for each sample and take the average during calculation of the quantum efficiency. Compared with P_c , P_b is almost negligible. Figure 2 shows the PL spectra P_c of different tetrapod samples. All the samples have the UV peak about 390 nm and have very weak defect emission in the visible region. The PL of the sample grown in optimal substrate temperature, Z3, is significantly stronger than the other three samples. The inset of Figure 2 shows the defect emission normalized with the UV peak of each sample. Z3 has the smallest defect to UV peak ratio (about 0.015), while the tetrapod grown in the highest temperature Z4 has the largest peak to peak ratio (about 0.05). This shows that Z4 has stronger defect emission than the other three samples, but it is still very weak to compare with the UV emission. As shown in Table I, Z3 has the highest absolute external quantum efficiency of 4.3% which is among the highest room temperature external quantum efficiency reported for nanostructured ZnO assemblies,⁷ while the other three samples vary from 1.9% to 2.4%. The external quantum efficiency of a ZnO crystal is only about 0.1% which is much smaller than that of the tetrapods. One may expect single crystal ZnO with less surfaces and ideal crystal structure should have comparable quantum efficiency with the ZnO tetrapods, however, the measured external quantum efficiency η is related to light extraction efficiency C_{ext} and internal quantum efficiency η_{int} (i.e., $\eta = C_{ext}\eta_{int}$). For the bulk ZnO crystal slab, only light within a small emission cone is able to escape into the air at the dielectric/air interface, the rest is total internally reflected within the bulk.

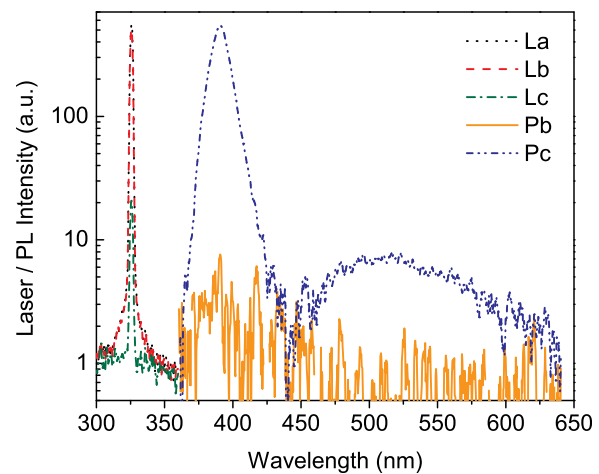


FIG. 1. Spectra of Z3 in the integrating sphere measurement in room temperature. At 325 nm, there are detected laser signals when the sphere was empty (L_a , black dotted line), the sample was placed inside with laser illuminated on the sphere wall (L_b , red dashed line), and laser illuminated on the sample (L_c , green dashed-dotted line). At 390 nm, there are detected PL when the sample was placed inside with laser illuminated on the sphere wall (P_b , orange solid line) and laser illuminated on the sample (P_c , blue dashed-dotted-dotted line).

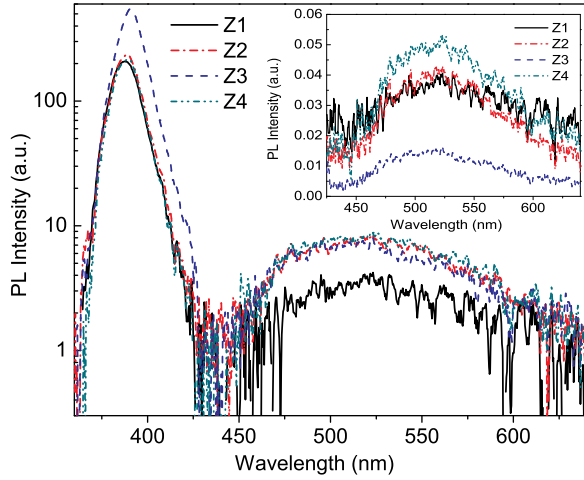


FIG. 2. PL spectra P_c of ZnO tetrapod samples Z1 (black solid line), Z2 (red dashed-dotted line), Z3 (blue dashed line), and Z4 (green dashed-dotted line) in integrating sphere measurement. Z3 has its PL significantly stronger than the other three samples. Inset shows the impurity emission normalized with the UV peak of each sample.

Most of these total internal reflection photons will be reabsorbed because of the large absorption coefficient for ZnO and large volume of the bulk sample, very few of these photons are able to escape into the air through the sample edge, thus, light extraction efficiency C_{ext} for the single crystal ZnO is very small. Furthermore, as shown in the time-resolved PL (see Fig. 3), the PL decay is very fast which indicate the dominant relaxation process for exciton in the ZnO crystal is by non-radiative recombination. For these reasons, the η of the ZnO crystal is very small (i.e., more than an order of magnitude smaller than the ZnO tetrapods). Indeed, recent work showed that individual isolated ZnO nanowires has η as large as 20% while closely packed assembly of nanowires has η of only $\sim 4\%$ (i.e., similar to our case) due to non-uniform excitation and possibly as a result of increasing reabsorption by the neighboring tetrapods.⁸ The reason why Z3 grown at growth temperature $\sim 930^\circ\text{C}$ exhibits the largest quantum efficiency is not fully understood. We believe it is partly due to some variation of structural properties of tetrapods in different growth temperature. The native defect concentrations are expected to be substrate temperature dependent, although in ZnO the temperature range for obtaining good crystal quality is unusually narrow. Nevertheless, our results are consistent with the PL measurement

TABLE I. The table shows the absolute external quantum efficiencies (η) of ZnO tetrapods Z1-Z4 and ZnO crystal obtained from integrating sphere PL measurement, ratio of the amplitudes of the fast to slow decay component A_1/A_2 , and decay time constants τ_1 and τ_2 calculated from the time-resolved measurement. $\tau = A_1\tau_1 + A_2\tau_2$ is the amplitude-weighted average decay time constant.

Sample No.	η (%) ± 0.1	A_1/A_2	τ_1 (ns)	τ_2 (ns)	τ (ns)
Z1	1.9	7.34 ± 1.07	2.9 ± 0.1	31.0 ± 0.5	6.3 ± 0.6
Z2	2.4	26.75 ± 4.47	2.4 ± 0.1	24.9 ± 0.5	3.2 ± 0.2
Z3	4.3	1.81 ± 0.09	5.7 ± 0.2	90.3 ± 2.3	35.9 ± 1.9
Z4	2.0	12.44 ± 2.05	2.6 ± 0.1	27.7 ± 0.4	4.5 ± 0.4
ZnO Crystal	0.1	2.90 ± 0.86	0.4 ± 0.1	1.0 ± 0.1	0.6 ± 0.1

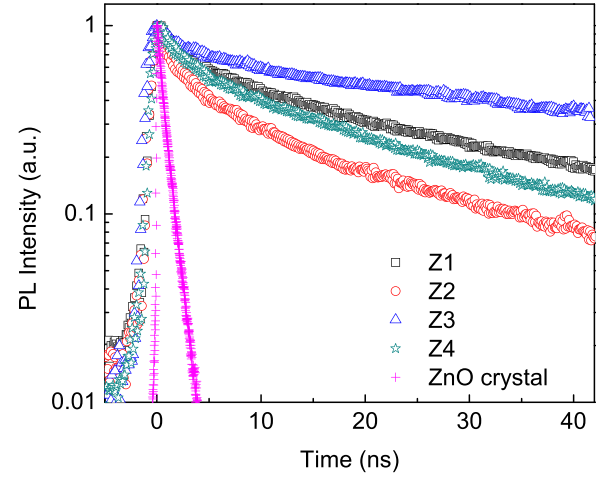


FIG. 3. Normalized PL decay curves of tetrapods Z1-Z4 and ZnO crystal in time-resolved measurement in room temperature. All curves exhibit bi-exponential decay behavior. ZnO crystal has PL lifetime much shorter than the tetrapods. Z3 has its PL lifetime significantly longer than Z1, Z2, and Z4.

reported in previous work,⁴ in which the tetrapod grown in optimal temperature has the strongest PL emission and weakest defect emission. The present results are also consistent with recent work on ZnO nanowires where again only a very narrow range of growth temperature one observe a large absolute quantum efficiency.⁸

The quantum efficiencies obtained in our tetrapods are comparable to the previous report in ZnO powders which were 0.02%–3.00% at room temperature depended on different particle sizes.⁷ According to Ref. 10, a mixture of ZnO tetrapod and nanowire has strong defect and weak UV emission if gaseous (air, dry argon, dry nitrogen, humid nitrogen) flow through the furnace during fabrication, but for humid argon the UV is much stronger. Hence our results also verify that in order to obtain strong UV and weak defect emission, suitable type of gas (humid argon) flowing through the furnace is important. Beside tetrapods, very few ZnO nanostructures can achieve such weak defect emission, and strong defect emission is common for ZnO nanomaterials.²

The time-resolved PL spectra at room temperature are shown in Figure 3. For the same reason as stated in the integrating sphere measurement above, we measured the time-resolved PL of 3 different regions for each sample and take the average when calculating of the decay time constants. Z3 has PL lifetime significantly longer than the other three samples. The decaying PL of all samples could not be fitted by a single-exponential curve, hence a bi-exponential fit was used instead. As demonstrated in measurement of individual tetrapods, the PL of isolated tetrapods can decay in single or double exponential manner.⁴ Thus, this double exponential decay in assembly of tetrapods is consistent with the previous measurements for ZnO nanostructures.^{4,12,13} The double exponential decay suggests distinct relaxation pathways or recombination in different regions of the structure such as from surface and bulk for the excited state recombination, although the exact mechanism is uncertain. This aspect of origin of the excited state recombination has been discussed in detail in our previous ZnO tetrapod work and other large gap semiconductor.^{4,14} Referring to Table I, the decay constants of Z3 are $\tau_1 = 5.7$ ns and

$\tau_2 = 90.3$ ns, which are considerably longer than the decay constants of the other three samples, especially for the slower decay constant τ_2 . The decay constants of ZnO crystal are $\tau_1 = 0.4$ ns and $\tau_2 = 1.0$ ns, which are much shorter than that of the tetrapods. The ratios of the amplitudes of the faster to slower decay component A_1/A_2 vary from 2 to 27. Among all tetrapods, Z3 has the smallest $A_1/A_2 = 1.81$ and which indicates it has the slow component contributing more in the decay process, while other samples have their fast components more dominating. The Z3 also has the slowest τ_1 and τ_2 among all samples measured. The results above show that for ZnO crystal with its very low quantum efficiency and fast PL lifetime, the non-radiative relaxation dominates the recombination process. On the other hand, the fact that Z3 has the largest quantum efficiency and the longest PL lifetime indicate that it should have a smaller non-radiative recombination rate than other samples, therefore, the excited state relaxation for Z3 is dominated by radiative recombination process.^{4,5}

For temperature dependent time-resolved measurement, the PL curve decays slower as temperature increases for all samples. Figure 4 shows the PL decay curves of Z3 in 7 K, 150 K, and 300 K. Again, the curves do not show single-exponentially decay. An amplitude-weighted average decay time constant $\tau = A_1\tau_1 + A_2\tau_2$ was calculated for each temperature instead. The plot of τ versus temperature for Z3 is shown in Figure 5. Qualitatively, the increase of decay lifetime with temperature can be explained as follows. First of all, radiative recombination of electron and hole (or exciton) in a semiconductor must follow momentum conservation law (i.e., $\Delta k = 0$). After excitation by a light source, the exciton transits to the conduction band. A temperature bath makes excitons dissociate from the bottom of the band and gain some momentum. Before recombination, they need to return to the bottom of the conduction band (i.e., in order to achieve $\Delta k = 0$). Their excess energy and momentum are dissipated as phonons. This dissociation effect of excitons becomes stronger as temperature increases, which also makes the radiative recombination lifetime increase. It is known that the radiative recombination coefficient for free

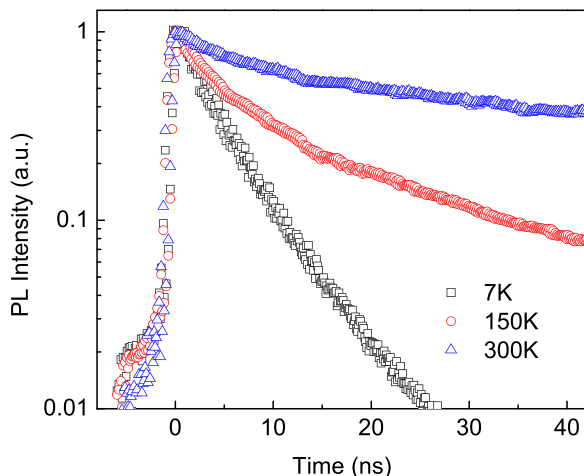


FIG. 4. Representative normalized PL decay curves of tetrapod Z3 in time-resolved measurement under different temperatures. PL curve decayed slower as temperature increases.

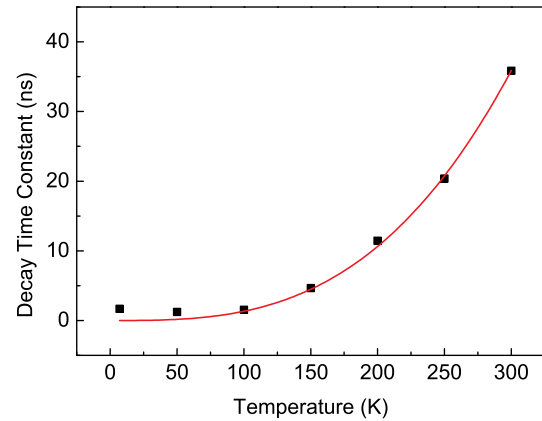


FIG. 5. Amplitude-weighted average decay time constant $\tau = A_1\tau_1 + A_2\tau_2$ calculated from experimental data (black points) in time-resolved PL and fitting curve (red line) as a function of temperature for Z3.

carrier and exciton in large bandgap semiconductors have the same $T^{-3/2}$ temperature dependence.¹⁵ However, ZnO has very large exciton binding energy, thus, exciton recombination should dominate even at room temperature.¹ For quantitative investigation, we attempt to test if our ZnO tetrapods results obey the theoretical model in Ref. 15 by simply fitting the experimental lifetime τ to the equation

$$\tau = aT^{\frac{3}{2}}, \quad (2)$$

where a is the fitting coefficient. The fitting curve is also shown in Figure 5. The average time constant data points are well fitted by Eq. (2) with $a = 2.66 \pm 0.06$ ns K^{-3/2}. Equation (2) is only strictly valid for temperature dependence for radiative recombination lifetime and this can only be calculated from the single exponential PL decay curve with the help of the measured QE. Thus, one has to extract some kind of effective lifetime from the double exponential decay in order to study the temperature dependence. Weighted average lifetime is a reasonable measure of the lifetime, although it is not strictly valid for Eq. (2), nevertheless, it should accurately mirror the change in exciton lifetime as a function of temperature. Indeed, good agreement of the experimental result to the theoretical prediction further prove that the weighted average lifetime reflect accurately the temperature dependence of the excited state radiative lifetime of the ZnO tetrapods. Fig. 5 shows that the increase in PL decay time constant with temperature further proves the decrease of radiative recombination rate and quantum efficiency with increasing temperature, which is consistent with the results in direct PL measurement. For ZnO crystal, although we still observed PL lifetime increases with increasing temperature, the rate of increase is much smaller compared to sample Z3 and the curve cannot be fitted to Eq. (2). This is also consistent with our earlier conclusion that recombination in a ZnO crystal is dominated by non-radiative process rather than radiative one.

IV. CONCLUSION

As a summary, integrating sphere measurements showed that the tetrapods have quantum efficiencies of 2%–4%. The

sample grown in optimal temperature, Z3, exhibited the largest external quantum efficiency ($\eta=4.3\%$) and longest PL decay lifetimes ($\tau_1=5.7$ ns and $\tau_2=90.3$ ns for fast and slow components) among all the samples. Our results give a further proof that precise control of grown temperature plays an important role in making high quality ZnO tetrapods. In time-resolved measurement under changing temperature, the amplitude-weighted average decay time constant versus temperature of Z3 is well fitted by the curve $\tau = aT^{\frac{3}{2}}$. This increase in PL lifetime with increasing temperature shows that the excited state relaxation process is dominated by radiative recombination.

ACKNOWLEDGMENTS

This work is partially supported by the Research Grants Council of Hong Kong (Project No. HKUST2/CRF/11 G).

¹Ü. Özgür, Y. I. Alivov, C. Liu, A. Teke, M. A. Reshchikov, S. Doğan, V. Avrutin, S.-J. Cho, and H. Morkoc, *J. Appl. Phys.* **98**, 041301 (2005).

²A. B. Djurišić and Y. H. Leung, *Small* **2**, 944 (2006).

³W. M. Kwok, A. B. Djurišić, Y. H. Leung, W. K. Chan, and D. L. Philips, *Appl. Phys. Lett.* **87**, 223111 (2005).

⁴Y. C. Zhong, A. B. Djurišić, Y. F. Hsu, K. S. Wong, G. Brauer, C. C. Ling, and W. K. Chan, *J. Phys. Chem. C* **112**(42), 16286 (2008).

⁵S. K. Lee, S. L. Chen, D. Hongxing, L. Sun, Z. Chen, W. M. Chen, and I. A. Buyanova, *Appl. Phys. Lett.* **96**, 083104 (2010).

⁶Y. Zhang, R. E. Russo, and S. S. Mao, *Appl. Phys. Lett.* **87**, 043106 (2005).

⁷M. Hauser, A. Hepting, R. Hauschild, H. Zhou, J. Fallert, H. Kalt, and C. Klingshirn, *Appl. Phys. Lett.* **92**, 211105 (2008).

⁸D. J. Gargas, H. Gao, H. Wang, and P. Yang, *Nano Lett.* **11**, 3792 (2011).

⁹A. B. Djurišić, Y. H. Leung, K. H. Tam, Y. F. Hsu, L. Ding, W. K. Ge, Y. C. Zhong, K. S. Wong, W. K. Chan, H. L. Tam, K. W. Cheah, W. M. Kwok, and D. L. Philips, *Nanotechnology* **18**, 095702 (2007).

¹⁰V. A. L. Roy, A. N. Djurišić, W. K. Chan, J. Gao, H. F. Lui, and C. Surya, *Appl. Phys. Lett.* **83**, 1 (2003).

¹¹J. C. De Mello, H. F. Wittmann, and R. H. Friend, *Adv. Mater.* **9**, 230 (1997).

¹²S. W. Jung, W. I. Park, H. D. Cheong, G.-C. Yi, H. M. Jang, S. Hong, and T. Joo, *Appl. Phys. Lett.* **80**, 1924 (2002).

¹³G. Xiang, U. Pal, and J. Garcia Serrano, *J. Appl. Phys.* **101**, 024317 (2007).

¹⁴Y. Zhong, K. S. Wong, W. Zhang, and D. C. Look, *Appl. Phys. Lett.* **89**, 022108 (2006).

¹⁵A. Dmitriev and A. Oruzhenikov, *J. Appl. Phys.* **86**, 3241 (1999).